Crystal Form and Orientation of Isotactic Polypropylene Samples Prepared by Vibration-Injection Molding

Jie Zhang, Tai Zeng, Ji Zhu, Yanwei Lei, Kaizhi Shen, Qiang Fu

Department of Polymeric Science and Engineering, Sichuan University, State Key Laboratory of Polymer Materials Engineering, Chengdu 610065, China

Received 20 August 2006; accepted 29 January 2007
DOI 10.1002/app.26554
Published online 12 July 2007 in Wiley InterScience (www.interscience.wiley.com).

ABSTRACT: A vibration–injection molding equipment was developed to prepare isotactic polypropylene injection samples to investigate their crystal form and orientation. Wide-angle X-ray scattering experiments (WAXD) were conducted in two modes: theta–theta mode and tube-fixed mode. Through vibration–injection molding, in additional to α form, β form, or γ form can be obtained under different conditions. At high melt temperature (230), β-PP can be induced and the core of the sample contains more β-PP than the surface. At low melt temperature (190), γ-PP can be induced and the core and the surface of the sample contain approximate same proportion of γ-PP. Pole figures show that α-PP of a static sample just orientates slightly along M direction, while that of vibration samples orientate much stronger. The orientation of the normal of (040)α plane of the sample obtained at $T = 230^{\circ}C$, $f = 0.5$ Hz, and $P_v = 75$ MPa is preferred in M direction, and the orientation of the normal of (040)α plane of the sample obtained at $T = 190^{\circ}C$, $f = 1.5$ Hz, and $P_v = 35$ MPa is preferred in N direction. β-PP and γ-PP do not show obvious orientation. © 2007 Wiley Periodicals, Inc. J Appl Polym Sci 106: 1456–1461, 2007

Key words: crystal form; orientation; isotactic polypropylene; vibration–injection; WAXD; pole figure

INTRODUCTION

The performance of semicrystalline polymer is decided directly by its final crystal structure and morphology. Isotactic polypropylene (I-PP) is a kind of semicrystalline polymer that has multicrystal forms. Under different crystallization conditions, the crystal form of I-PP may be α-PP, β-PP, or γ-PP, and different crystal form has different properties. For example, β-PP has a better ability of impact resistance than α-PP.[1–3] At the same time, crystal orientation is a key factor that influences the properties of I-PP products. Therefore, there were some studies using pole figures on the crystal orientation of injection-molded polypropylene compounds,[4] polypropylene sheets produced by die-drawing and rolling,[5–7] and extruded tubular film of I-PP.[8]

Oscillation or vibration technique has been used in injection molding to control the molecular orientation and crystal morphology to enhance the mechanical performance of PP.[9–12] However, there has been little emphasis on crystal form and orientation, especially on the orientation of different crystal forms of I-PP samples prepared by oscillation or vibration injection molding. In this article, self-designed vibration–injection molding equipment was used to prepare I-PP samples, and WAXD and pole figure were used to characterize their crystal form and orientation.

EXPERIMENTAL

Material

I-PP F401 used in the experiment was commercialized products from Yan Shan petroleum chemical, Beijing, China, $M_w = 7.8 \times 10^4$, MFI = 1.87 g/min.

Samples preparation and characterization

A pressure vibration–injection machine with vibration frequency of 0 ~ 1.5 Hz and vibration pressure of 0 ~ 75 MPa was developed to prepare I-PP samples. During injection and packing, a pulsation pressure was introduced to the melt in a mold cavity to causes the melt vibrating forth and backwards with certain frequency and pressure. Three parameters, including melt temperature (T), vibration frequency (f), and vibration pressure (P_v) that represents the

Correspondence to: K. Shen (zhaolanr@163.com).
Contract grant sponsor: National Natural Science Foundation of China; contract grant numbers: 50473053, 50533050.
Contract grant sponsor: National Basic Research Program of China; contract grant number: 2005CB623800.
Contract grant sponsor: Scientific Research Foundation for Returned Overseas Chinese Scholars, State Education Ministry.

TABLE I
Processing Parameters in Vibration Injection Molding

Processing parameters	Parameters value
Injection pressure (MPa)	40
Packing pressure (MPa)	40
Melt temperature (°C)	190/230
Mould temperature (°C)	80
Vibration pressure (MPa)	0–75
Frequency (Hz)	0–1.5

maximum value of the pulsation pressure, were changed in our experiment. The method and equipment were introduced in detail in our previous articles.[12,13] The processing parameters are listed in Table I.

The wide-angle X-ray scattering experiments (WAXD) were conducted using a Brvker D8 diffractometer. The wavelength of the monochromated X-ray from CuKa radiation was 0.154 nm and the scanning 2θ range was from 5° to 30° with a scanning rate of 1°/min. We used two modes to do the experiments, theta-theta mode and tube-fixed mode. When theta-theta mode was used, both tube (X-ray source) and detector scanned at the same rate. When tube-fixed mode was used, the tube was fixed at an angle of 1° while detector scanned. Because of the same depth that X-ray could penetrate into a sample, the result of theta-theta mode contains more information of the core of samples and the result of tube-fixed mode contains more information of the surface of samples. The scan direction was the flow direction. The data for pole figure were obtained using the same instrument with a texture attachment.

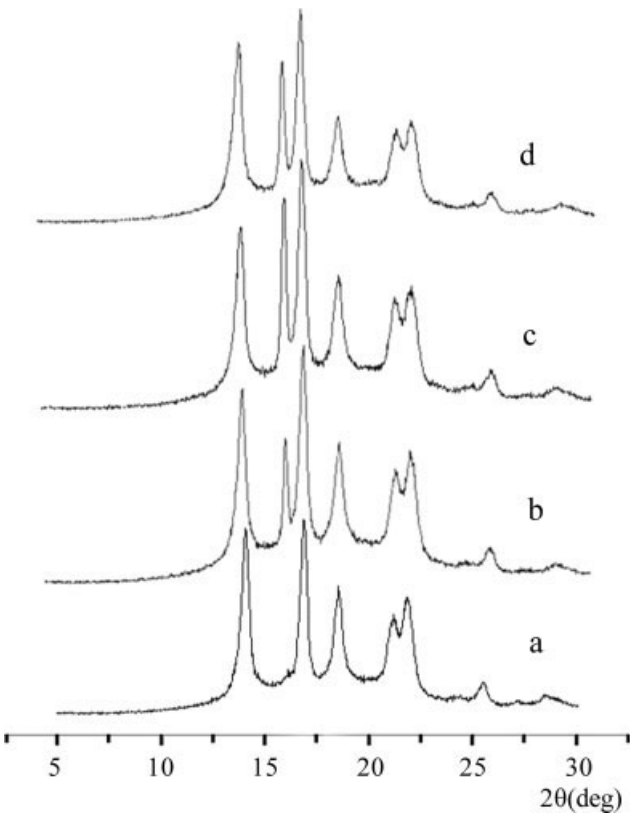

Figure 1 WAXD of samples obtained at 230°C by theta-theta mode. (a) Static sample, (b) f = 0.5 Hz, P_v = 35 MPa, (c) f = 0.5 Hz, P_v = 75 MPa, (d) f = 1.5 Hz, P_v = 35 MPa.

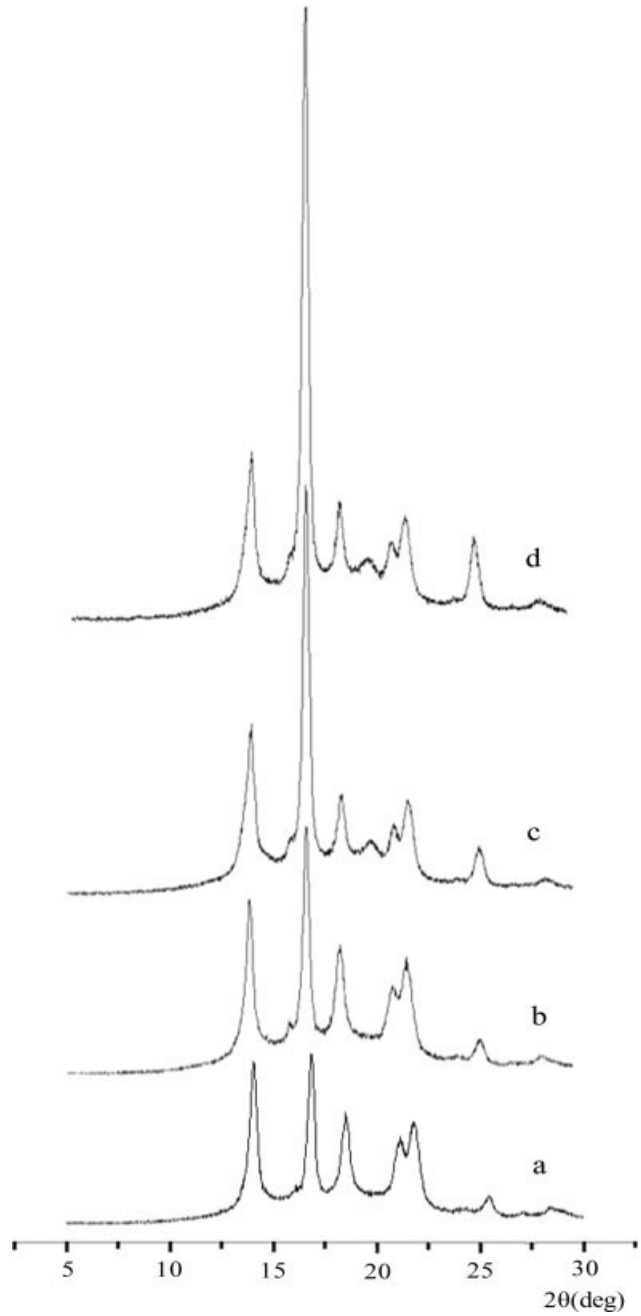

Figure 2 WAXD of samples obtained at 190°C by theta-theta mode. (a) Static sample, (b) f = 0.5 Hz, P_v = 35 MPa, (c) f = 0.5 Hz, P_v = 75 MPa, (d) f = 1.5Hz, P_v = 35 MPa.

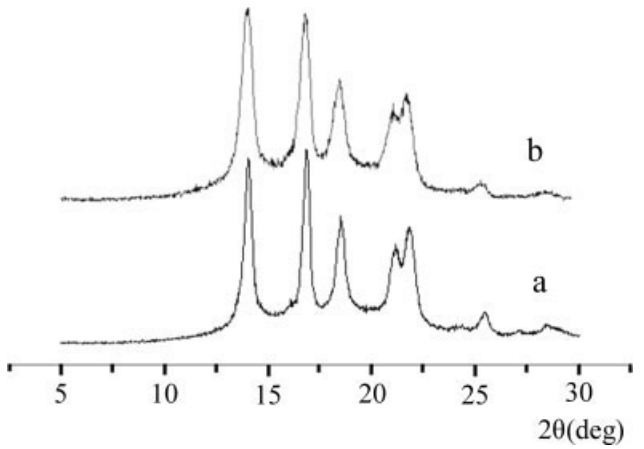

Figure 3 WAXD of static sample. (a) Theta-theta mode, (b) tube-fixed mode.

EXPERIMENT RESULTS

WAXD

WAXD diagrams can be used to determine crystal forms of I-PP samples. The data used in Figures 1 and 2 were obtained using theta-theta mode. When melt temperature is 230°C, the α-ipp is formed under conventional injection condition as shown in Figure 1(a). However, one observes another diffraction peak (300) at $2\theta = 16.5^\circ$ from other diagrams in Figure 1, which is the characteristic peak of β-PP. It indicates that β-PP can be induced through vibration at 230°C. The intensity of the peak is related to vibration pressure and frequency. When both vibration pressure and frequency are low [Fig. 1(b)], the intensity is low, and it increases as increasing the two parameters.

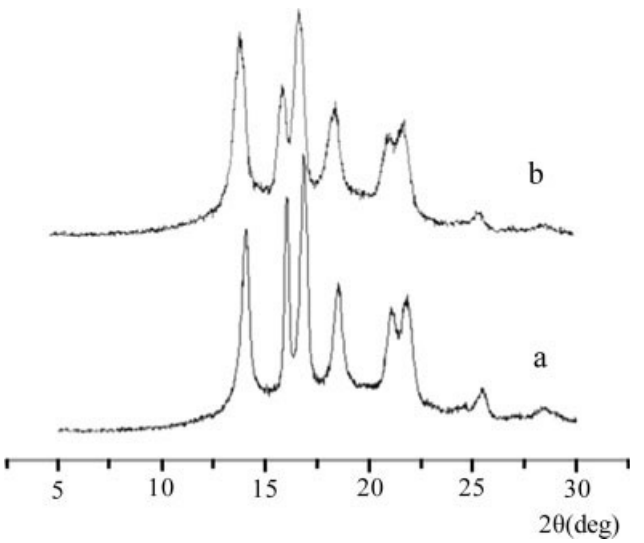

Figure 4 WAXD of sample obtained at $T = 230$°C, $f = 0.5$ Hz, and $P_v = 75$ MPa. (a) Theta-theta mode, (b) tube-fixed mode.

According to the intensity of the peaks, the relative content of β-phase can be obtained as follows:[14]

$$k = \frac{H_\beta}{H_\beta + (H_{\alpha 1} + H_{\alpha 2} + H_{\alpha 3})}$$

where $H_{\alpha 1}$, $H_{\alpha 2}$, $H_{\alpha 3}$ are intensities of α-diffraction peaks corresponding to (040)α, (110)α, (130)α, respectively, and H_β is the intensity of the $(300)_\beta$. Therefore, the content of β-phase is 0.19, 0.30, and 0.24 corresponding to Figure 1(b–d). It means that more β-PP can be formed at high vibration pressure compared with high frequency in the range of our experiment.

Figure 2 shows the WAXD diagrams of I-PP samples obtained by vibration-injection molding at 190°C. Instead of the peak at $2\theta = 16.5^\circ$, there is a small peak at $2\theta = 20.1^\circ$ in Figure 2(c,d). It means that no β-PP but γ-PP is induced at this temperature. No change of crystal form is seen at low vibration

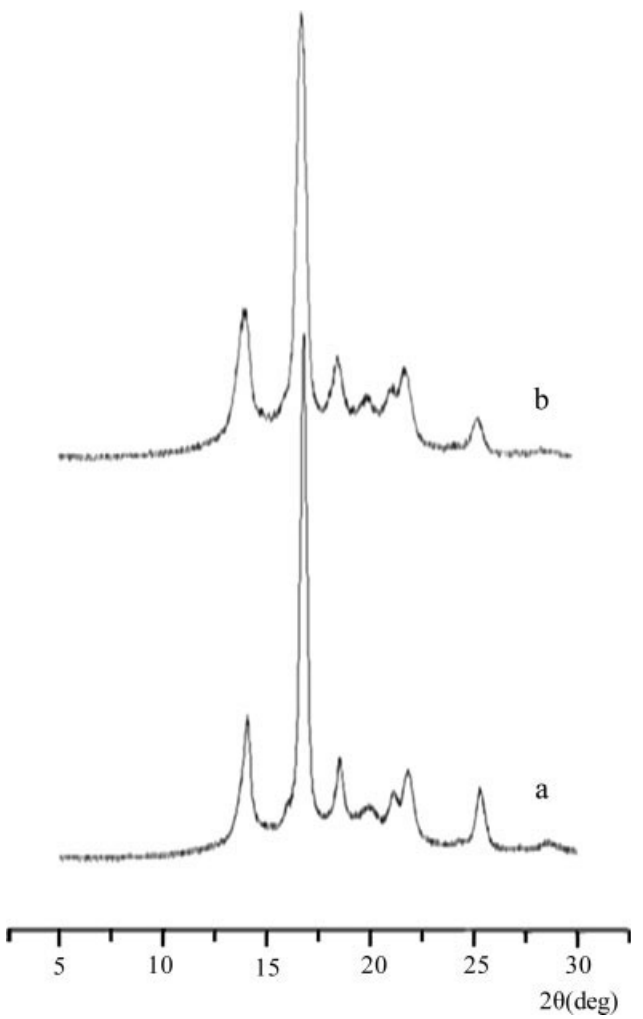

Figure 5 WAXD of sample obtained at $T = 190$°C, $f = 1.5$ Hz, and $P_v = 35$ MPa. (a) Theta-theta mode, (b) tube-fixed mode.

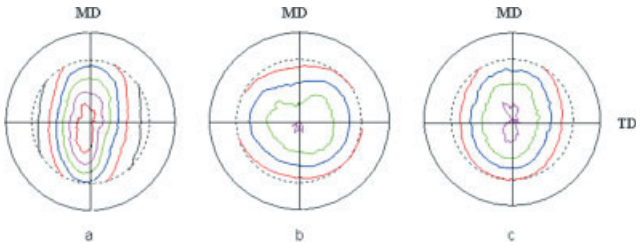

Figure 6 Pole figures of α-PP of static sample. (a) (040) plane, (b) (110) plane, (c) (130) plane. [Color figure can be viewed in the online issue, which is available at www.interscience.wiley.com.]

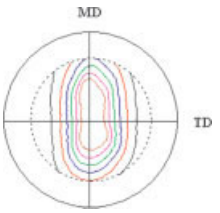

Figure 8 Pole figure of (300) plane of β-PP. Sample obtained at the same conditions as Figure 7. [Color figure can be viewed in the online issue, which is available at www.interscience.wiley.com.]

frequency and low vibration pressure [Fig. 2(b)]. One should note that the (040)α peak becomes very strong in Figure 2(c,d), due to the high frequency or high pressure processing condition.

Figures 3–5 are comparisons of results between theta-theta mode and tube-fixed mode. There is no obvious difference between the two diagrams in Figure 3. It indicates that the crystal form and the orientation of the core of static sample are almost the same as those of the surface. However, the peaks of the diagram obtained using theta-theta mode are narrower than those of the diagrams obtained using tube-fixed mode, and it can be found in the other two figures. It seems that crystals in the core are more perfect than those in the surface. Compared with diagram b, the peak at $2\theta = 16.5^\circ$ of diagram a is much higher and the (040)α peak is stronger in Figure 4. It means that the core of the sample contains more β-PP than the surface of the sample, the proportions are 0.3 and 0.17, respectively. In Figure 5, although the intensity of (040)α peaks of diagram a and b is not the same, the intensity of the peak at $2\theta = 20.1^\circ$ is almost the same. It seems that the core and the surface of the sample contain approximately the same proportion of γ-PP.

Pole figure

Figure 6 is pole figures of (040)α, (110)α, (130)α reflection of the static sample. The normal of (040)α represents the b axis of α monoclinic, the (040)α pole figure actually exhibits the orientation for b axis. In Figure 6(a), the inner contour has the strongest pole intensity, and the contours are ellipses with small ratios of major axis to minor axis. The contours of Figure 6(b,c) are almost circular at large angles. It indicates that the b-axis of the static sample just orientates slightly along M direction (MD).

Figure 7 is pole figures of(040)α, (110)α, (130)α reflection of the sample obtained at $T = 230^\circ$C, $f = 0.5$ Hz, and $P_v = 75$ MPa. The (040) poles have a stronger equatorial orientation than that shown in Figure 6(a), and it is evident that the b-axis is arranged in a cylindrical manner about the MD. At the same time, b-axis has a slight preference orientation about N direction (ND), as there are not any closed contours in the center in the pole-figure. As shown in Figure 7(b), the pole intensity of (110)α plane has the biggest value in the center of the equator, the ND orientation of (110) normal is obvious. In Figure 7(c), the direction of the pole intensity is along MD. Since (130)α plane is parallel to the c-axis of α monoclinic, the normal of (130) is perpendicular to the c-axis. It is regarded that the c-axis has a preferential orientation in T direction (TD).

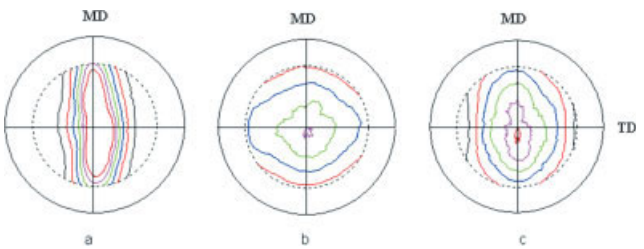

Figure 7 Pole figures of α-PP of sample obtained at $T = 230^\circ$C, $f = 0.5$ Hz, and $P_v = 75$ MPa. (a) (040) plane, (b) (110) plane, (c) (130) plane. [Color figure can be viewed in the online issue, which is available at www.interscience.wiley.com.]

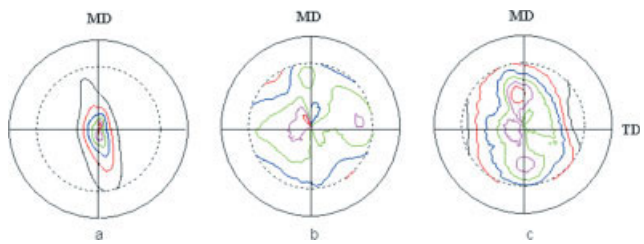

Figure 9 Pole figures of α-PP of sample obtained at $T = 190^\circ$C, $f = 1.5$ Hz, and $P_v = 35$ MPa. (a) (040) plane, (b) (110) plane, (c) (130) plane. [Color figure can be viewed in the online issue, which is available at www.interscience.wiley.com.]

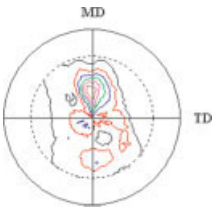

Figure 10 Pole figure of (117) plane of γ-PP. Sample obtained at the same conditions as Figure 9. [Color figure can be viewed in the online issue, which is available at www.interscience.wiley.com.]

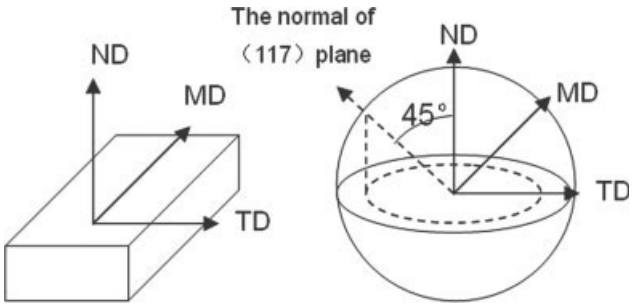

Figure 11 A schematic drawing of the orientation of the normal of (117) plane of γ-PP.

Figure 8 shows the $(300)_\beta$ reflection of the sample used in Figure 7. Similar with (040)α of static sample, the poles of the reflection plane of the peak neither approach uniaxial orientation about MD nor preferentially orientate along ND. Obviously, $(300)_\beta$ plane does not have a preferential orientation at the processing condition used. It is relative to the thermodynamics stability of β-PP.

The sample used in Figure 9 was obtained at T = 190°C, f = 1.5 Hz, and P_v = 35 MPa. From Figure 9(a), the density of the closed contours becomes very high in the center, and few contours cross the excircle. At this condition, the (040) poles show maximum intensities in the ND. As there is no contours cross the excircle in the direction perpendicular to MD, it is not pronounced that the b-axis is primarily oriented along the equatorial bands. It indicates that the b-axis rotates around the ND in a cylindrical manner with a rotating angle between the b-axis and the basic circle below 90°. Comparing (110)α and (130)α in Figure 9 with (110)α and (130)α in Figure 7, it can be found that the pole intensity points are more disperse. Therefore, when melt temperature is 190°C, increasing vibration frequency induce (040)α to arrange parallel to the surface of the sample bar. However, (110)α and (130)α which are parallel to the c-axis do not show preferential orientation in MD or TD, respectively.

Figure 10 shows the (117)γ reflection of the sample used in Figure 9. The pole figure shows that the normal of (117) plane does not orientate in an obvious manner. More or less the concentrated closed contours indicates that most poles point the direction which form a 45°angle between the normal and ND, which is shown in Figure 11.

DISCUSSION AND CONCLUSION

In the process of traditional injection molding, polymer melt flows into a mold cavity through a runner system under the action of injection pressure, which causes polymer molecular chains to align along flow direction to form orientation. However, because of the slow cooling of polymer melt, especially the melt in the core of samples, molecular chains orientated have the tendency of recovering the state of disorder. Therefore, the orientation degree of crystals is low. When there is a vibration field added, it develops a pulsation force on polymer melt in the cavity. The force produces a press-and-release effect on the melt due to its viscoelasticity. So, there are continuous periodical shear stresses during both stages of injection and packing that can induce the change of crystal form and crystal orientation of I-PP samples.

Through vibration–injection molding, by changing the processing parameters, such as melt temperature, vibration frequency and vibration pressure, β form or γ form can been obtained in I-PP samples, in additional to α form. At high melt temperature (230°C), β form can be induced. The content of β-PP increases as increasing vibration frequency and vibration pressure, and the content of β-PP of the core of the sample is higher than that of the surface. At low melt temperature (190°C), γ-form can be induced, and the core and the surface of the sample contain approximate same proportion of γ-PP. Because the core of a sample has longer time to crystallize, the crystals in the core are more perfect than those in the surface.

Pole figures show that α-PP of a static sample just orientates slightly along MD, while that of vibration samples orientate much stronger. The orientation of the normal of $(040)_\alpha$ plane of the sample obtained at T = 230°C, f = 0.5 Hz, and P_v = 75 MPa is preferred in MD, and the orientation of the normal of $(040)_\alpha$ plane of the sample obtained at T = 190°C, f = 1.5 Hz, and P_v = 35 MPa is preferred in ND. β-PP and γ-PP do not show obvious orientation.

We would like to express our great thanks to Mr. John Harper and Dr. David Ross, IPTME, Loughborough University, UK, for doing pole figure experiments.

References

1. Varga, J. J Macromol Sci Phys 2002, 41, 1121.
2. Premphet, K.; Horanont, P. J Appl Polym Sci 1999, 74, 3445.

3. Tjong, S.C.; Shen, J. S.; Li, R. K. Y. Polym Eng Sci 1996, 36, 100.
4. Chen, Z.; Finet, M. C.; Liddell, K. J Appl Polym Sci 1992, 46, 1429.
5. Chaffey, C. E.; Taraiya, A. K.; Ward, I. M. Polym Eng Sci 1997, 37, 1773.
6. Hibi, S.; Takahiro, N. Polym Eng Sci 1995, 35, 902.
7. Hibi, S.; Takahiro N.; Jun, M. Polym Eng Sci 1995, 35, 911.
8. Choi, D.; White, J. L. Polym Eng Sci 2001, 41, 1743.
9. Kalay, G.; Allan, P.; Bevis, M. J. Plast. Rubb. Proc. Appl. 1995, 23, 71.
10. Kalay, G.; Bevis, M. J. J Polym Sci Part B: Polym Phys 1997, 35, 241.
11. Ibar, J. P. Polym Eng Sci 1998, 38, 1.
12. Zhang, J.; Shen, K. J Polym Sci Part B: Polym Phys 2004, 42, 2385.
13. Zhang, J.; Shen, K. J Appl Polym Sci 2005, 96, 818.
14. Karger-Kocsis, J. Polypropylene: Structure, Blends and Composites; Chapman & Hall: London, 1995.